molecular pharmaceutics

articles

Stearic Acid-*g*-chitosan Polymeric Micelle for Oral Drug Delivery: In Vitro Transport and in Vivo Absorption

Hong Yuan,* Lin-Juan Lu, Yong-Zhong Du, and Fu-Qiang Hu

College of Pharmaceutical Science, Zhejiang University, 388 Yuhangtang Road, Hangzhou 310058, P. R. China

Received August 29, 2010; Revised Manuscript Received November 26, 2010; Accepted December 6, 2010

Abstract: Stearic acid-*g*-chitosan (low molecular weight chitosan CS-SA) with different amino-substituted degrees was synthesized and evaluated as an oral delivery vehicle in this paper. Synthesized CS-SA with 4.47%, 24.36% and 40.36% amino-substituted degree (SD) could form micelles by self-aggregation in aqueous medium. The critical micelle concentration (CMC) ranged from about 0.16 to 0.25 mg/mL, which decreased with the increased SD of CS-SA. The CS-SA micelles had 33.4−130.9 nm size and 22.9− 48.4 mV zeta potential. CS-SA with higher SD had the smaller size and the higher zeta potential. The permeability and possible transport route of CS-SA micelles across the gastrointestinal tract was investigated by in vitro model Caco-2 cells. The results exhibited that the CS-SA micelles had good permeability, and the permeability enhanced with increasing SD of the CS-SA. The transport of the micelles showed energy, pH and concentration dependent transcytosis process, mainly through macropinocytosis and partly via fluid-phase transcytosis and caveolar route. The reversible decrease in transepithelial electrical resistance (TEER) by treatment of micelles suggested that paracellular transport pathway was another route of the micelles crossing the gastrointestinal tract. Using doxorubicin (DOX) as a model drug, the permeation results further demonstrated that the DOX transport mediated by CS-SA micelles could avoid efflux via P-glycoprotein. In vivo study demonstrated that the micelles could significantly improve the bioavailability of encapsulated drug. The results presented that the CS-SA with higher SD was a promising vehicle for oral drugs.

Keywords: Chitosan; micelles; amino-substitution degree; Caco-2 cells; P-glycoprotein; oral delivery

1. Introduction

During the past decade there has been a growing interest in the investigation of polymeric micelles as a potential carrier for drug delivery.[1−3] Polymeric micelles usually have a hydrophobic core surrounded by a hydrophilic outer shell.[1] The inner hydrophobic core of the polymer has a large capacity to accommodate hydrophobic drugs,[2] while the hydrophilic shell allows retaining the stability of polymeric micelle in an aqueous environment.[4] Compared to surfactant micelles the polymeric micelles are less prone to dissociation at low concentrations and thus could maintain the micellar structure that facilitates prolonged circulation in the bloodstream.[3] This is mainly because the polymeric micelles usually form through self-assembly at a low concentration,

* Corresponding author. Mailing address: College of Pharmaceutical Science, Zhejiang University, 388 Yuhangtang Road, Hangzhou 310058, P. R. China. Tel (fax): 86-571-88208439. E-mail: yuanhong70@zju.edu.cn.

(1) Nishiyama, N.; Kataoka, K. Current state, achievements, and future prospects of polymeric micelles as nanocarriers for drug and gene delivery. *Pharmacol. Ther.* **2006**, *112*, 630–648.

(2) Nakanishi, T.; Fukushima, S.; Okamoto, K.; Suzuki, M.; Matsumura, Y.; Yokoyama, M.; Okano, T.; Sakurai, Y.; Kataoka, K. Development of the polymer micelle carrier system for doxorubicin. *J. Controlled Release* **2001**, *74*, 295–302.

(3) Rijcken, C. J. F.; Soga, O.; Hennink, W. E.; van Nostrum, C. F. Triggered de-stabilisation of polymeric micelles and vesicles by changing polymers polarity: An attractive tool for drug delivery. *J. Controlled Release* **2007**, *120*, 131–148.

(4) Discher, D. E.; Eisenberg, A. Polymer vesicles. *Science* **2002**, *297*, 967–973.

10.1021/mp100289v
Published on Web 12/07/2010

called the critical micelle concentration (CMC). They were originally developed and used for intravenous (iv) administration. But recently their application in oral administration has also been extensively investigated.[5−7] It is notably for polymeric micelles due to the fact that polymeric micelles exhibit lower CMC, which offer greater resistance toward dissociation upon dilution in the GI tract.[8] Besides, the large drug loading capacity of the hydrophobic core of the polymeric micelles helps greatly increase the drug absorbed through the GI mucosa and reaches the blood circulation at concentrations above the therapeutic threshold.[3] The hydrophilic shell help increase the solubility of the drug and protect it from degradation in the GI tract. Currently, some synthetic bioadhesive polymers are investigated as GI delivery vehicles by achieving an intimate contact with the mucosa. They reduce presystemic drug metabolism,[9] prolong the residence time at the site of drug action or absorption and provide a steep concentration gradient at the absorption membrane. The polymers include PEG, cellulose derivatives such as HPC and chitosan.[8,10]

Being a muco/bioadhesive polymer, chitosan is considered a good candidate for an oral drug delivery vehicle.[11] In addition to the well-known advantages such as low toxicity, excellent biocompatibility and degradability,[12] chitosan itself possesses antibacterial activity.[13] The antibacterial activity of chitosan could be due to the electrostatic interactions between the amine groups of chitosan and the anionic sites on the bacterial cell wall. Chitosan, by controlling its molecular weight or deacetylated degree, could effectively provide a controlled release of the candidate drug.[8,11]

In recent years, many researchers focused on water-soluble chitosan with lower molecular weight, to synthesize chitosan hydrophobic derivatives for the delivery of several antitumor drugs.[14,15] In our previous research, the lower molecular weight chitosan named CSO hydrophobic derivative stearic acid-*g*-CSO (CSO-SA) was synthesized via the coupling reaction by using EDC.[16,18] The CSO-SA micelles have been used as the gene delivery vehicle, which showed higher in vitro gene transfection efficiency.[16] The paclitaxel loaded CSO-SA micelles realized a controlled drug release by the shell cross-link of CSO-SA.[17] Further studies found that the CSO-SA micelles could be rapidly uptaken by tumor cells,[23] and in vivo study showed that the antitumor activity of doxorubicin was greatly improved by conjugating the drug with the CSO-SA micelles.[18] Based on this research, this study was aimed at exploring the potential of CS-SA micelles used in oral administration. The permeability investigation was performed by using Caco-2 cells,[19] a well-recognized in vitro model for permeability estimation of intestinal absorbed drugs. They were also exploited to elucidate the cell penetration mechanisms and P-gp efflux pump effluence of the CS-SA micelles.[20] In vivo study was carried out in order to further evaluate the pharmacokinetic properties of the micelles.

2. Experimental Section

2.1. Materials. Chitosan (M_w = 450 kDa, 95% deacetylated degree) was supplied by Yuhuan Marine Biochemistry

(5) Mathot, F.; van Beijsterveldt, L.; Preat, V.; Brewster, M.; Arien, A. Intestinal uptake and biodistribution of novel polymeric micelles after oral administration. *J. Controlled Release* **2006**, *111*, 47–55.

(6) Sant, V. P.; Smith, D.; Leroux, J. C. Enhancement of oral bioavailability of poorly water-soluble drugs by poly (ethylene glycol)-block-poly(alkyl-acrylate-co- methacrylic acid)self-assemblies. *J. Controlled Release* **2005**, *104*, 289–300.

(7) Gaucher, G.; Satturwar, P.; Jones, M. C.; Furtos, A.; Leroux, J. C. Polymeric micelles for oral drug delivery. *Eur. J. Pharm. Sci.* **2010**, *76*, 147–158.

(8) Francis, M. F.; Cristea, M.; Winnik, F. M. Polymeric micelles for oral drug delivery: why and how. *Pure Appl. Chem.* **2004**, *76*, 1321–1335.

(9) Gaucher, G.; Dufresne, M. H.; Sant, V. P.; Kang, N.; Maysinger, D. J.; Leroux, C. Block copolymer micelles: preparation, characterization and application in drug delivery. *J. Controlled Release* **2005**, *109*, 169–188.

(10) Grabovac, V.; Guggi, D.; Bernkop-Schnurch, A. Comparison of the mucoadhesive properties of various polymers. *Adv. Drug Delivery Rev.* **2005**, *57*, 1713–1723.

(11) Hejazi, R.; Amiji, M. Chitosan-based gastrointestinal delivery systems. *J. Controlled Release* **2003**, *89*, 151–165.

(12) Lee, E.; Lee, J.; Lee, I. H.; Yu, M.; Kim, H.; Chae, S. Y.; Jon, S. Conjugated chitosan as a novel platform for oral delivery of paclitaxel. *J. Med. Chem.* **2008**, *51*, 6442–6449.

(13) Hernandez-Lauzardo, A. N.; Bautista-Banos, S.; Velazquez-del Valle, M. G.; Mendez -Montealvo, M. G.; Sanchez-Rivera, M. M.; Bello-Perez, L. A. Antifungal effects of chitosan with different molecular weights on in vitro development of Rhizopus stolonifer (Ehrenb: Fr.) Vuill. *Carbohydr. Polym.* **2008**, *73*, 541–547.

(14) Opanasopit, P.; Ngawhirunpat, T.; Chaidedgumjorn, A.; Rojanarata, T.; Apirakaramwong, A.; Phongying, S.; Choochottiros, C.; Chirachanchai, S. Incorporation of camptothecin into N-phthaloyl chitosan-mPEG self-assembly micellar system. *Eur. J. Pharm. Biopharm.* **2006**, *64*, 269–276.

(15) Zhang, C.; Ping, Q. N.; Zhang, H. Self-assembly and characterization of paclitaxe- loaded N-octyl-O-sulfate chitosan micellar system. *Colloids Surf., B* **2004**, *39*, 69–75.

(16) Hu, F. Q.; Zhao, M. D.; Yuan, H.; You, J. A novel chitosan oligosaccharide-stearic acid micelles for gene delivery: properties and in vitro transfection studies. *Int. J. Pharm.* **2006**, *315*, 158–166.

(17) Hu, F. Q.; Ren, G. F.; Yuan, H.; Du, Y. Z.; Zeng, S. Shell cross-linked stearic acid grafted chitosan oligosaccharide self-aggregated micelles for controlled release of paclitaxel. *Colloids Surf., B* **2006**, *50*, 97–103.

(18) Hu, F. Q.; Liu, L. N.; Du, Y. Z.; Yuan, H. Synthesis and antitumor activity of doxorubicin conjugated stearic acid-g-chitosan oligosaccharide polymeric micelles. *Biomaterials* **2009**, *30*, 6955–6963.

(19) Camenisch, G.; Alsenz, J.; vande Waterbeemd, H.; Folkers, G. Estimation of permeability by passive diffusion through Caco-2 cell monolayers using the drugs' lipophilicity and molecular weight. *Eur. J. Pharm. Sci.* **1998**, *6*, 313–319.

(20) Van der Sandt, I.C. J.; Blom-Roosemalen, M.C M.; Boer, A. G.; Breimer, D. D. Specificity of doxorubicin versus rhodamine-123 in assessing P-glycoprotein functionality in the LLC-PK1, LLC-PK1:MDR1 and Caco-2 cell lines. *Eur. J. Pharm. Sci.* **2000**, *11*, 207–214.

Co., Ltd. (Zhejiang, China). Stearic acid was purchased from Shanghai Chemical Reagent Co., Ltd. (China). Chitosanase was purchased from Dyadic International, Inc. (USA). Doxorubicin hydrochlorate (DOX·HCl) was gifted from Hisun Pharm Co., Ltd. (China). 1-Ethyl-3-(3-dimethylaminopropyl)carbodiimide (EDC) was purchased from shanghai Medpep Co., Ltd. (China). Verapamil was purchased from Pharmaceutical and Biological Products laboratory (China). 2,4,6-Trinitrobenzene sulfuric acid (TNBS), 3-(4,5-dimethylthiazol-2-yl)-2,5-diphenyltetrazolium bromide (MTT), and fluorescein isothiocyanate (FITC) were purchased from Sigma Chemical Co. (USA). *N*-2-Hydroxyethylpiperazine-*N*-2-ethanesulfonic acid (HEPES) was purchased from Sigma Saint Quentin Fallavier (France). Rhodamine B was purchased from Amresco, Co. (USA). BCA protein assay kit was purchased from Beyotime Institute of Biotechnology (Haimen, Jiangsu, China). RPMI 1640 medium, Dulbecco's modified Eagle's medium (DMEM, high-glucose), fetal bovine serum (FBS), nonessential amino acids, 0.25% trypsin−EDTA solution and antibiotic−antimycotic were purchased from Gibco BRL (USA). All other chemicals were analytical or chromatographic grade.

2.2. Synthesis and Characterization of CS-SA. To synthesize CS-SA chemical conjugate, chitosan (CS) was first obtained by enzymatic degradation from chitosan. The time of hydrolysis was controlled by molecular weight measurement of chitosan, and the molecular weight of final chitosan (CS) was determined by gel permeation chromatography (GPC) with TSK-gel column (G3000SW, 7.5 mm i.d. × 30 cm) at 25 °C. Master samples of polysaccharide with different molecular weight (M_w 5.9, 11.8, 22.8, 47.3,112, 212 kDa) were dissolved in acetate buffer solution (pH 6.0, the mobile phase), and their final concentrations were set to 1.0 mg/mL. A calibration curve was performed by means of polysaccharide samples using the integral molecular weight distribution method. The weighted lyophilized powder of CS was dissolved in acetate buffer solution (pH 6.0) with a final concentration of 1.0 mg/mL of the sample and was chromatographed with a flow rate of 0.8 mL/min. The molecular weight of CS was then calculated from the calibration curve.

The CS-SA copolymer was then synthesized via the reaction of carboxyl groups of SA with amine groups of CS in the presence of EDC.[21] Briefly, 2 g of CS was dissolved 140 mL of distilled water and heated up to 60 °C. Different amounts of SA (15%, 30% or 50% relating with the molar number of glucosamine unit in CS) and EDC (ten times the molar number of SA) were dissolved in 70 mL of an ethanol/acetone mixture (ethanol/acetone = 2/5, v/v). After stirring for 1 h at 400 rpm, 60 °C, the solution was added into CS aqueous solution, followed by stirring for another 24 h. Finally, the reaction solution was dialyzed against DI water using a dialysis membrane (MWCO: 3.5 kDa, Spectrum Laboratories, Laguna Hills, CA) for two days, and the reaction solution was lyophilized. Then the lyophilized product was further purified with ethanol to remove the byproduct. Finally, the product CS-SA with different charged amount of SA (15%, 30% and 50%) was redispersed in DI water and lyophilized, and the products were labeled as CS-SA-1, CS-SA-2 and CS-SA-3, respectively. The charged amount of SA was calculated as follows:

$$\text{charged amount of SA} = \{(W_{SA} \times M_{CSO})/(W_{CSO} \times N_{NH2} \times M_{SA})\} \times 100\ \% \quad (1)$$

where W_{SA} and W_{CS} were the mass of SA and CS, M_{CS} and M_{SA} were the molecular weight of CS and SA, and N_{NH2} was 28, representing the number of amino groups of one molar CS (5 kDa).

The amino-substitution degree (SD) for CS-SA conjugate was determined by using a 2,4,6-trinitrobenzene sulfonic acid (TNBS) test.[16,18] Simply, 1 mg/mL CS-SA micelles solution was prepared as the stock solution. Then 200 μL of stock solution was added into 2 mL of $NaHCO_3$ (4%, w/v) and 2 mL of 0.1% TNBS mixture solution. The mixture was incubated at 37 °C for 2 h, followed by the addition of 2 mL of HCl (2 N). The final reaction mixture was measured at 344 nm by a spectrophotometer (TU-1800PC, Beijing Purkinje General Instrument Co., Ltd., China). The degrees of amino-substitution for CS-SA were calculated using SD % process software.

The critical micelle concentration (CMC) of the synthesized CS-SA was estimated by fluorescence spectroscopy using pyrene as a probe. A fluorometer (F-2500, HITACHI Co., Japan) was used to record fluorescence spectra, the excitation wavelength was 337 nm, and the slits were set at 2.5 nm (excitation) and 10 nm (emission). The intensities of the emission were monitored at a wavelength range of 360−450 nm. The concentration of CS-SA micelle solutions containing 5.93×10^{-7} M pyrene was varied from 5.0×10^{-3} to 1.0 mg/mL. Then the ratio of the intensities (I_1/I_3) of the first peak (I_1, 374 nm) to the third peak (I_3, 385 nm) was calculated.

2.3. Preparation of Doxorubicin (DOX) Loaded CS-SA Micelles. DOX was obtained by the reaction of doxorubicin hydrochloride (DOX·HCl) with twice molar numbers of triethylamine (TEA) in dimethyl sulfoxide (DMSO) overnight,[22] and used for the preparation of DOX loaded CS-SA (CS-SA/DOX) micelles. First, 20 mg of CS-SA was dissolved in 10 mL of DI water, followed by the addition of 0.4 mL of DOX−DMSO solution (1 mg/mL). After dialysis against DI water using a dialysis membrane (MWCO: 3.5 kDa, Spectrum Laboratories, Laguna Hills, CA) for 24 h,

(21) Huang, M.; Ma, Z.; Khor, E.; Lim, L. Y. Uptake of FITC-chitosan nanoparticles by A549 cells. *Pharm. Res.* **2002**, *19*, 1488–1494.

(22) Kohori, F.; Yokoyama, M.; Sakai, K.; Okanob, T. Process design for efficient and controlled drug incorporation into polymeric micelle carrier systems. *J. Controlled Release* **2002**, *78*, 155–163.

(23) Hu, F. Q.; Wu, X. L.; Du, Y. Z.; You, J.; Yuan, H. Cellular uptake and cytotoxicity of shell cross-linked stearic acid-grafted chitosan oligosaccharide micelles encapsulating doxorubicin. *Eur. J. Pharm. Biopharm.* **2008**, *69*, 117–125.

the product was centrifuged at 3000 rpm for 8 min to remove precipitated drug and the final product was obtained.

The DOX content encapsulated in CS-SA micelles was measured by fluorescence spectrophotometer (F-2500, HITACHI Co., Japan). The excitation wavelength, emission wavelength and slit openings were set at 505, 565, and 5 nm, respectively. The drug encapsulation efficiency (EE) and drug loading (DL) of CS-SA/DOX were assayed by the centrifugal-ultrafiltration method. A CS-SA/DOX solution of 0.4 mL was added into centrifugal-ultrafiltration tubes (Microcon YM-10, MWCO 3000, Millipore Co., USA) and centrifuged at 10,000 rpm for 20 min. The DOX concentration (C_u, μg/mL) in ultrafiltrate was measured by fluorescence spectrophotometer. Another 0.4 mL of CS-SA/DOX solution was diluted 100-fold by DMSO aqueous solution (DMSO/H_2O = 9:1, v/v) to dissociate the CS-SA micelles. The DOX concentration (C_f, μg/mL) in diluted solution was measured, and was considered as the total drug amount in 0.4 mL of CS-SA/DOX solution. The drug encapsulation efficiency (EE, %) and drug loading (DL, %) of CS-SA/DOX could be calculated by the following equations:

$$\mathrm{EE}\ \% = (C_f \times 100 - C_u) \times V/M_a \times 100\ \% \quad (2)$$

$$\mathrm{DL}\ \% = (C_f \times 100 - C_u) \times V/[800 + (C_f \times 100 - C) \times V] \times 100\ \% \quad (3)$$

where M_a is the charged amount of drug, and the unit is microgram; V is the total volume of CS-SA/DOX solution, and the unit is milliliter.

2.4. Characterization of CS-SA and CS-SA/DOX Micelles. *2.4.1. Size and Zeta Potential.* Micellar size and zeta potential of CS-SA micelles and CS-SA/DOX micelles with the concentration of 1 mg/mL CS-SA were performed using a Zetasizer analyzer (3000 HS, Malvern Instruments Ltd., U.K.). All measurements were performed in triplicate.

2.4.2. TEM Observation. The morphological examinations of the CS-SA micelles and COS-SA/DOX micelles were performed by transmission electron microscopy (TEM) (JEOL JEM-1230, Japan). The samples were stained with 2% (w/v) phosphotungstic acid and placed on copper grids with films for viewing by TEM.

2.5. In Vitro Release Studies. In vitro release studies of DOX from CS-SA micelles were performed using phosphate-buffered saline (PBS, pH 7.2) as the dissolution medium. The saturated solubility of DOX in pH 7.2 PBS was measured to be 76 μg/mL. Briefly, 1 mL of CS-SA/DOX micelle solution was added into dialysis filter (M_w: 3.5 kDa) and put in a plastic tube containing 20 mL of PBS (pH 7.2) solution. The plastic tube was then placed in an incubator shaker (HZ-8812S, Scientific and Educational Equipment plant, Tai Cang, China), which was maintained at 37 °C and shaken horizontally at 65 rpm. At predetermined time intervals, a 0.1 mL sample was withdrawn and replaced with 1 mL of fresh PBS solution. The drug concentration was determined by fluorescence spectrophotometer. All drug release tests were performed thrice.

2.6. Stability of CS-SA Micelles Exposed in Different pH Conditions. Taking into account that the micelles were developed as delivery vehicles for oral administration drugs and the specialty of gastrointestinal pH circumstances, it was desired to evaluate their stability under these conditions. Consequently, CS-SA micelles with different SD % were incubated in simulated intestinal medium with different pH conditions (pH = 7.4, pH = 6.8, pH = 5.9). Samples were prepared and the mean particle size of the micelles was determined by PCS at certain time intervals (0, 2, 3, 5, 7 days).

2.7. Characterization of Caco-2 Cell Monolayer. *2.7.1. Cell Culture.* Caco-2 (human intestinal epithelial cell) cells were cultured in Dulbecco's modified Eagle's medium (DMEM) supplemented with 10% (v/v) FBS (fetal bovine serum), 1% (v/v) glutamine, penicillin (100 U/mL), streptomycin (100 U/mL), and 1% nonessential amino acids (NEAA).

2.7.2. Integrity of Caco-2 Cell Monolayer. Caco-2 cells were seeded at a density of 6.0×10^5 cells/cm^2 and cultured on polycarbonate filter membranes with a pore size of 0.4 μm and a surface area of 1.13 cm^2 (Costar Transwell, Millipore Corp., Bedford, MA, USA). The culture medium was changed every other day in the first two weeks and every day in the following week. The integrity of the cell monolayer was checked by measuring the transepithelial electrical resistance (TEER) values and monitoring the permeability of the paracellular leakage marker Lucifer yellow (LY) across the monolayer. The TEER value was measured by using a Millicell-ERS volt-ohmmeter (Millipore Co., USA), LY was determined in a Tecan Spectrofluor fluorescence plate reader at an excitation wavelength of 485 nm and an emission wavelength of 535 nm. TEER was measured at different time intervals. The intrinsic resistance of the system (insert alone) was subtracted from the total resistance (cell monolayer plus insert) to yield the monolayer resistance. The resistance value was expressed as $\Omega \cdot \mathrm{cm}^2$. Completely differentiated cells used in transport assay were cultured for 21 days.

2.7.3. P-gp Function Detection. The P-glycoprotein (P-gp) function of Caco-2 cell monolayer was evaluated by examining Rhodamine B (Rho B) permeation ability.[25] The concentration of Rho B used was 5 μM, which was dissolved in HBSS solution. Analysis of Rho B was carried out by fluorescence spectrometer (Ex = 485 nm, Em = 535 nm, slit = 5 nm). Apparent permeability coefficient (P_{app}) was calculated from the slope of the accumulated amount versus time curve, and the value was determined using Eq as follows:

(24) Panyam, J.; Zhou, W. Z.; Prabha, S.; Sahoo, S. K.; Labhasetwar, V. Rapid endo-lysosomal escape of poly(D,L-lactide-co-glycolide) nanoparticle; Implication for drug and gene delivery. *J. FASEB* **2002**, *16*, 1217–1226.

(25) Paruchuri, V. K.; Nguyen, A. V.; Miller, J. D. Zeta-potentials of self assembled surface micelles of ionic surfactants adsorbed at hydrophobic graphite surfaces. *Colloids Surf., A* **2004**, *250*, 519–526.

$$P_{app} = (dQ/dt)/3600 \times A \times C_0 \quad (4)$$

where dQ/dt was determined from the amount of Rho B appearing in the basolateral compartment or apical side (Q) over time (t/h) during the experiment, A was the surface area of the porous membrane ($A = 1.13$ cm^2), and C_0 represented the initial concentration of Rho B in the donor side.

The ratio of P_{app} (absorption-secretion) was determined by the following equation:

$$P_{ratio} = P_{app,bl\text{-}ap}/P_{app,ap\text{-}bl} \quad (5)$$

where $P_{app,bl\text{-}ap}$ was the apparent permeation coefficient from the basolateral to the apical side (blood to intestine) (cm/s) and $P_{app,ap\text{-}bl}$ was the apparent permeation coefficient from the apical to the basolateral side (intestine to blood) (cm/s).

2.8. Cell Viability of CS-SA Micelles. Toxicity of CS-SA micelles against Caco-2 cells was performed by MTT assay. Briefly, 200 μL of cell suspension was seeded in 96-well micro titer plates and allowed to adhere for 48 h to reach confluence. Cells were treated with CS-SA micelles diluted with HBSS solution (HEPES 25 mM, pH 7.4) at various concentrations (25−600 μg/mL) for 4 h at 37 °C. After 4 h incubation, the medium was removed. 100 μL of MTT (1.0 mg/mL in HBSS, pH 7.4) was added to each well, and the cells were incubated at 37 °C for another 4 h. MTT medium was then pipetted off from the wells, and the formazan crystals were dissolved in 200 μL of DMSO, with shaking for 10 min to achieve complete dissolution. Absorption was measured at 570 nm in a micro plate reader (Bio-Rad, model 680, U.S.A.). The viability was presented as the percent of sample well to the control well using cells without treatment. Each concentration of the samples had three replicates. The reading taken from the wells with cells cultured with control medium was used as 100% viability value. The cell viability was calculated as $A_{sample}/A_{control} \times 100\%$.

2.9. Preparation of FITC Labeled CS-SA Micelles. FITC labeled CS-SA micelles (FITC-CS-SA) was synthesized using a previous method.[22] Briefly, 100 mg of CS-SA was dissolved in 10 mL of DI water and followed by dropwise addition of 4 mL of FITC ethanol solution (2 mg/mL). The mixture solution reaction was carried out for 8 h at room temperature, and then, after dialysis against DI water for 24 h, the final product was obtained.

2.10. Transport Study. *2.10.1. Transport Study of FITC-CS-SA Micelles across Caco-2 Cell Monolayer.* For the transport assay of CS-SA micelles, the culture medium was replaced by transport medium HBSS solution (0.5 mL to apical side (AP) and 1.5 mL to basolateral side (BL)) and the cells were allowed to equilibrate for 30 min. After the transport medium was discarded, 0.5 mL of FITC-CS-SA HBSS solution was applied to the apical (AP) side followed by addition of 1.5 mL of HBSS solution to the basolateral side. At preset time intervals, solution in basolateral (BL) side was collected and rapidly replaced with equivalent fresh HBSS solution. The content of FITC-CS-SA transported was detected by fluorescence spectrometer (Ex = 497 nm, Em = 523 nm, slit = 5 nm). Transport tests were conducted using different incubation temperatures (4, 25 and 37 °C), pH of incubation medium (pH 5.9, 6.8 and 7.4) and concentrations of CS-SA (75, 150, and 300 μg/mL).

The inhibition transport assay was conducted for 4 h by using different blocking conditions: (i) sodium azide (0.1% w/v) for 1 h, (ii) 10 μg/mL of chlorpromazine for 30 min, (iii) 1 μg/mL of colchicines for 30 min, (iv) 450 mM of sucrose for 1 h, (v) 50 mM of ammonium chloride; the concentrations adopted were chosen based on previous studies.[21,24]

Given that a paracellular pathway might be another route of the micelles across the cell monolayer, TEER was detected during CS-SA micelle treatment. After removal of the culture medium, the Caco-2 cell monolayers were treated with CS-SA micelles (0.6 mg/mL) for 240 min at the apical compartment. Then the TEER variation of cell monolayers was measured using the Millicell-ERS system (Millipore, USA). As a comparison, TEER of cells incubated with blank HBSS solution was detected at the same time intervals. After 4 h of treatment, the micelle solution was removed and the cells were incubated with a fresh cell culture medium (DMEM). The recovery of TEER values was monitored for 2, 4, 8, 12, and 24 h after the treatment.

2.10.2. Transport Study of DOX Loaded CS-SA Micelles. The transport study of DOX CS-SA/DOX micelles was conducted in a similar procedure as FITC-CS-SA micelles, and the DOX·HCl solution was used as a control. Transport of DOX was carried out in both directions, and the concentration used was certificated to have no toxic effect on the cells.

2.11. Cellular Uptake Investigation. To deeply understand the mechanism of micelle endocytosis via Caco-2 cells, the uptake study was conducted at different conditions: (i) treated at different temperatures, 37 and 4 °C; (ii) treated with different inhibitors as described in section 2.10.1, and the uptake was conducted for 1 h.

Investigation of CS-SA/DOX micelles uptake in Caco-2 cells was mainly aimed at the P-gp efflux pump effluence on the CS-SA micelles, which relied on the fact that DOX was a typical P-gp substrate.[20]

The qualitation observation was viewed by fluorescence microscope (Leica, DMIL, DM 3000, Germany), while the content of CS-SA and DOX taken up by Caco-2 cells was measured by fluorescence spectrometer. After certain time intervals, cells were washed twice with PBS and then harvested. The cell lysate was centrifuged at 8,000 rpm for 15 min, and the protein content inside the cell was measured using the Micro BCA protein assay kit. The cellular uptake percentage of DOX was calculated from the following equation:

$$\text{DOX uptake percentage } (\%) = C_t/C_{t0} \times 100\% \quad (6)$$

where C_t and C_{t0} were the intracellular DOX concentration corrected by intracellular protein concentration at t time and t_0 time, respectively.

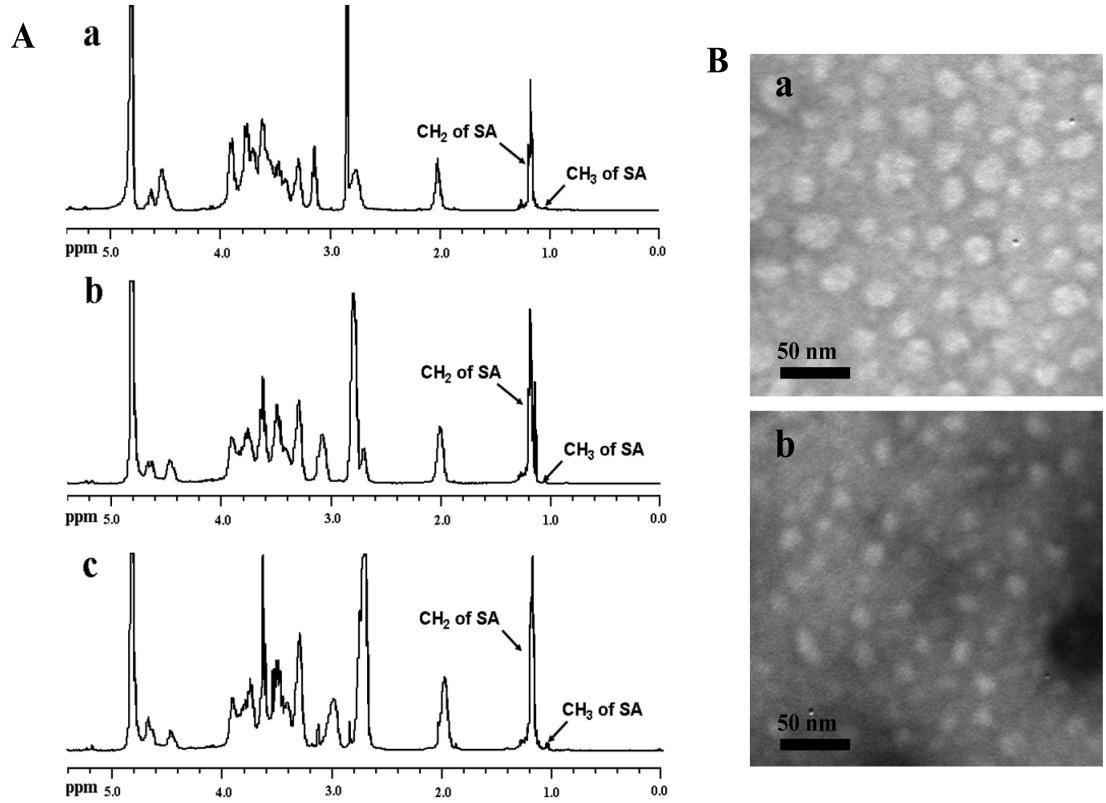

Figure 1. (A) ^{1}H NMR spectra of CS-SA-1 (a), CS-SA-2 (b), and CS-SA-3 (c); the important peaks were pointed out. (B) TEM images of CS-SA-3 micelles (a) and CS-SA-3/DOX micelles (b).

2.12. In Vivo Pharmacokinetics of CS-SA/DOX Micelles. For the in vivo studies, male Sprague−Dawley rats (200−210 g body weight) were used. The rats were fasted 16 h before experiment but had free access to water, and were divided into three sets (three rats per set). After tail intravenous injection or oral administration with a dose of 12 mg of DOX/kg, 1 mL blood samples were taken at different time intervals. Prior to analysis, an equal volume of acetonitrile was added to a 1 mL plasma sample for deproteinization. The mixture was vortexed for 30 s and centrifuged at 8,000 rpm for 10 min. Then, 1 mL of the supernatant was transferred to the colorimetric cylinder, and DOX concentrations in the samples were measured. The pharmacokinetic parameters of DOX after intravenous or oral administration were obtained from the plasma concentration−time curve by applying pharmacokinetic analysis software, DAS 2.1.1. The area under the plasma concentration versus time curve up to the last measured time (AUC_{0-t}) was calculated by using the linear trapezoidal rule, using kinetic data collected from individual values. The absolute bioavailability was calculated from the dose corrected areas under the curves for oral versus intravenous administration. All values are expressed as the mean ± SD.

The protocol of animal study was approved by the Institutional Animal Care and Use Committee (IACUC), Zhejiang University of China.

2.13. Statistical Analysis. All the experiments were conducted in triplicate, and the results were compared using a t test. Values of $p < 0.05$ and $p < 0.01$ were considered statistically significant and highly significant, respectively.

3. Results

3.1. Synthesis of CS-SA and Preparation of DOX Loaded CS-SA Micelles. Molecular weight of the obtained CS was measured by gel permeation chromatography. The CS-SA was synthesized by using CS with average molecular weight of 5 kDa. The structure of synthesized CS-SA chemical conjugate was confirmed from the ^{1}H NMR spectrum shown in Figure 1A. The properties of synthesized CS-SA are shown in Table 1. From Table 1, it was found that the SD of CS-SA increased with increasing the charged amount of SA. Due to the hydrophobic SA modification of water-soluble CS molecules, the synthesized CS-SA could self-aggregate to form micelles. The CMC of CS-SA was assessed by fluorescence spectroscopy using pyrene as a probe. As seen from Table 1, the micelles with higher SD had smaller micellar size, which might result from the increasing hydrophobic interaction among SA chains. The zeta potential was increased with increasing SD. Definitely, the increase of SD led to the small amount of primary amino group in the CS-SA molecule. However, the CS-SA micelles with high SD had smaller size than that of CS-SA micelles with low SD. And it was supposed that the surface zeta potential of the micelles reflected the surface charge density.

Table 1. Properties of Synthesized CS-SA Micelles and Prepared DOX Loaded CS-SA Micelles[a]

blank and DOX loaded micelles	SD (%)	CMC (μg/mL)	d_n (nm)	PI	ζ (mV)	EE (%)	DL (%)
CS-SA-1	4.47 ± 1.01	246.9	130.9 ± 18.2	0.08 ± 0.02	22.9 ± 0.7		
CS-SA-2	24.36 ± 0.35	218.43	66.2 ± 7.9	0.42 ± 0.01	32.0 ± 0.5		
CS-SA-3	40.36 ± 0.64	161.85	33.4 ± 2.8	0.46 ± 0.02	48.4 ± 1.1		
CS-SA-1/DOX			66.0 ± 0.9	0.36 ± 0.06	29.3 ± 0.1	70.94 ± 1.51	11.82 ± 0.25
CS-SA-2/DOX			38.2 ± 1.5	0.59 ± 0.02	38.0 ± 0.9	66.38 ± 1.84	11.06 ± 0.31
CS-SA-3/DOX			28.1 ± 3.1	0.60 ± 0.04	46.4 ± 2.3	76.15 ± 6.31	12.69 ± 1.05

[a] SD: amino-substitution degree of the micelles. PI: polydispersity index of the micelle size. CMC: critical micelle concentration in DI water solution. EE: encapsulation efficiency. DL: drug loading ability. d_n: number average diameter. ζ: zeta potential. Data represent the mean ± standard deviation ($n = 3$).

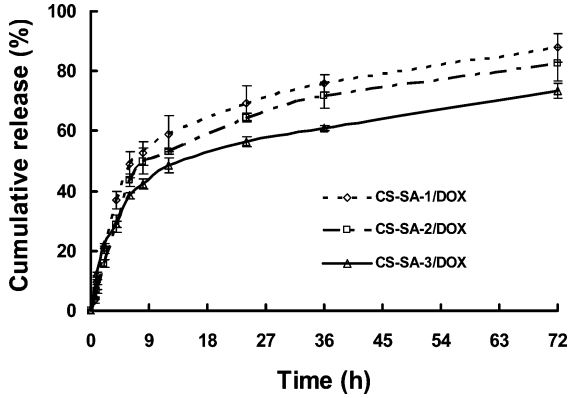

Figure 2. In vitro release profile of DOX from CS-SA micelles.

The smaller size which meant larger surface area would have higher surface charge density and thus a higher surface zeta potential.[25]

Using DOX as a model drug, The CS-SA/DOX was prepared by the dialysis method. The properties of CS-SA/DOX are also presented in Table 1. After the DOX loading, the micellar size became smaller; however, the zeta potential indicated no significant change. Using the dialysis method, the EE of CS-SA/DOX micelles was above 65%, and the DL could reach up to 11%.

Figure 1 presented the TEM images of CS-SA-3 micelles and CS-SA-3/DOX micelles. It was observed that both micelles indicated spherical morphologies, and sizes close to the number average diameter obtained from the determination of Zetasizer analyzer. Overall, the size after drug loading was decreased compared with blank micelles. The causes were mainly attributed to the mechanism of the CS-SA micelle aggregation. The hydrophobic chain of stearic acid had weak hydrophobic interaction compared with other hydrophobic polymers, and the hydrophilic chain of chitosan was difficult to fold compared with PEG and other hydrophilic chains. After drug loading, the cohesive force of the hydrophobic interaction was enhanced and thus caused the decrease of the size.[23]

3.2. In Vitro Release Study. As shown in Figure 2, the release behavior of DOX was delayed as the graft ratio of SA in CS-SA micelles, while there was slight difference in the first 24 h. At 0.5 h, the percentage of DOX released from the CS-SA micelles with different SD value were found in the range 3.15−5.46%. With time prolonged, more drugs released from the carrier, and at time point 72 h, the cumulative drug released percentage reached the range 73−87%, respectively. The lower drug release rate was found in CS-SA/DOX micelles with higher DOX content.

3.3. Stability of CS-SA Micelles Exposed to Different pH Conditions. To ensure delivery of the carried drug to its site of absorption, the micellar carrier must be able to maintain stability when exposed to the different pH conditions of the GI tract. Accordingly, we have monitored the size of the micelles with different SD value after incubation in gastrointestinal fluids at different pH conditions (Figure 3). As presented in Figure 3, in the gastric medium with series pH conditions, the micelles presented a different size variation with prolonged incubation time. Generally, the micelles appeared stable during the first three days incubation, and the size distribution was in a narrow range (PI < 0.5). The stability was influenced both by the amino substitution of the micelles and by the pH condition of the incubation medium. Overall, relatively smaller size was found of the micelles with higher SD and in the medium with lower pH. The size of CS-SA-3 micelles was mainly maintained in the range 22.8−74.7 nm, while CS-SA-1 and CS-SA-2 micelles were located in the range 33.1−164.3 nm and 75.2−204.5 nm, respectively.

3.4. Assessment of Cell Monolayer Integrity and Investigation on Influences of Temperature, Medium pH and Micelle Concentration. Cell monolayer integrity was controlled by measurement of transepithelial electrical resistance (TEER) and by evaluation of cell permeability to Lucifer yellow.[26,28] TEER of Caco-2 cell monolayer was increased with prolonged incubation time (Figure 4A) and was often used after 21 days culture on polycarbonate inserts.[27] As the results present, the TEER value reached to about 800 $\Omega \cdot cm^2$ after 21 day culture and the apparent

(26) Sandri, G.; Bonferoni, M. C.; Rossi, S.; Ferrari, F.; Gibin, S.; Zambito, Y.; Colo, D. G.; Caramella, C. Nanoparticles based on N-trimethylchitosan: Evaluation of absorption properties using in vitro (Caco-2 cells) and ex-vivo (excised rat jejunum) models. *Eur. J. Pharm. Biopharm.* **2007**, *65*, 68–77.

(27) Behrens, I.; Kissel, T. Do cell culture conditions influence the carrier-mediated transport of peptides in Caco-2 cell monolayers? *Eur. J. Pharm. Sci.* **2003**, *19*, 433–442.

(28) Moyes, S. M.; Morris, J. F.; Carr, K. E. Culture conditions and treatments affect Caco-2 characteristics and particle uptake. *Int. J. Pharm.* **2010**, *387*, 7–18.

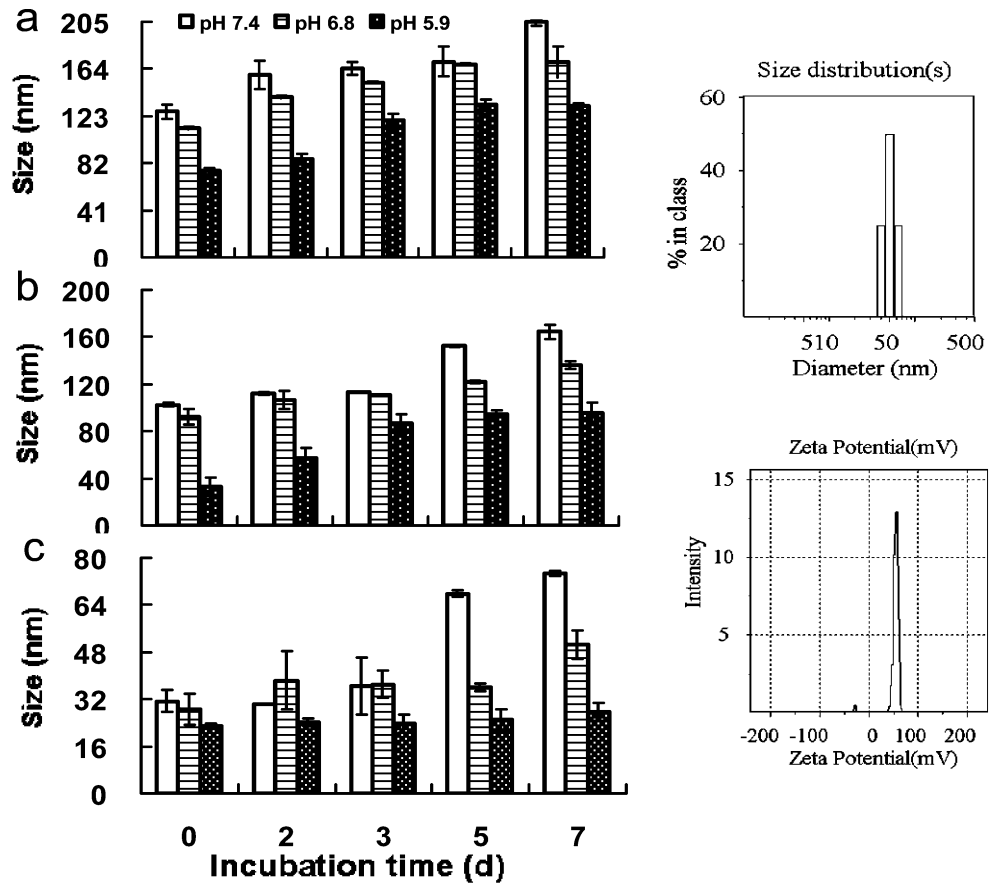

Figure 3. Stability of CS-SA-1 (a), CS-SA-2 (b), and CS-SA-3 (c) micelles in simulated gastric fluid with different pH conditions (mean ± SD, $n = 3$).

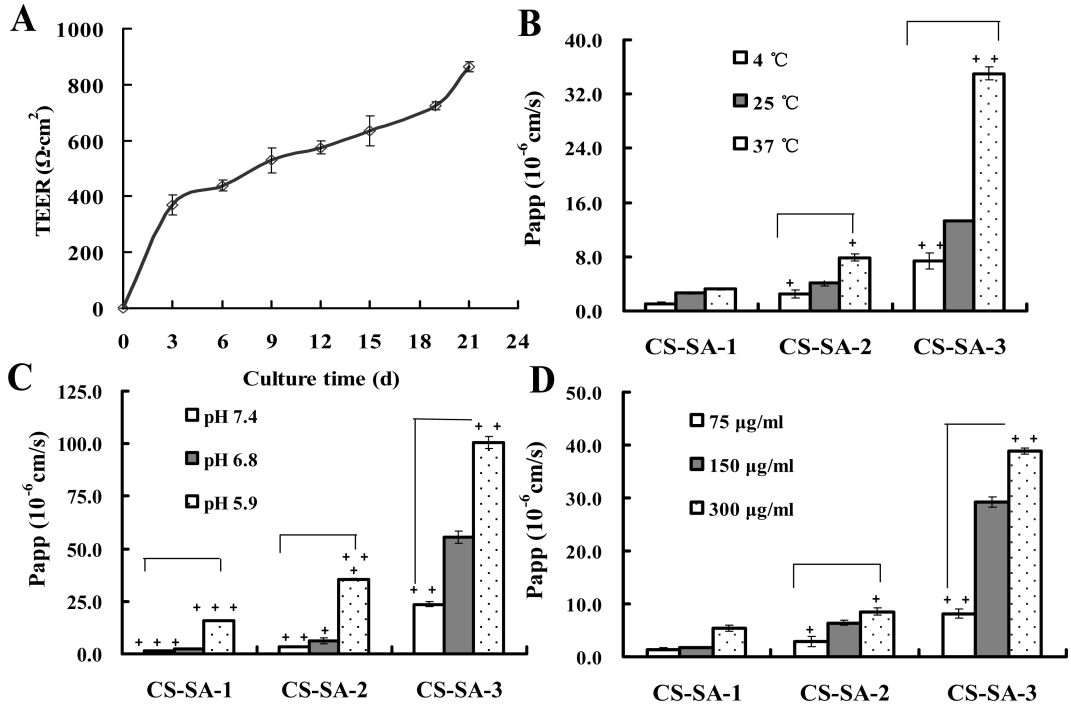

Figure 4. (A) Variation of TEER value of Caco-2 Cell monolayer against culture time. (B) Apparent permeability coefficient (P_{app}) of CS-SA micelles under different incubation temperature. (C) Different medium pH and (D) different CS-SA concentration. + and ++, +++ represent $P < 0.05$ and $P < 0.01$, respectively.

permeability coefficient (P_{app}) for Lucifer yellow was 0.23 $\times$ 10^{-6} cm/s, which was considered tight enough for the transport experiments according to previous investigation.[29]

For the permeation study of CS-SA micelles, the micelle concentrations were fixed at 150 μg/mL for the energy and pH dependent assay. No fluorescence was found in the basolateral chamber containing FITC free solution. Therefore, the fluorescence intensity detected in the basolateral side was attributed to the micelles. From Figure 4B, it clearly showed that the permeability of the micelles was increased with the incubation temperature. At 4 °C, the permeation of micelles was inhibited and the permeation coefficient ($P_{app,}$ cm/s) of all micelles was low, from 1.071 $\times$ 10^{-6} to 7.36 $\times$ 10^{-6} cm/s (lowest of CS-SA-1 to highest of CS-SA-3 micelles). Whereas, at 37 °C, the permeability was significantly enhanced for all micelles, P_{app} values were increased to 3.28 $\times$ 10^{-6} to 3.50 $\times$ 10^{-5} cm/s, which was 3−5 times higher than that under 4 °C.

The pH value of incubation medium was also an important factor that might affect the permeation behavior of drug in oral administration. To imitate all possible physiological pH conditions in the intestinal tract in vivo (pH 5.0−8.0),[28] the apical pH with 5.9, 6.8, and 7.4 was applied, while the basolateral pH was kept constant at pH 7.4. It was found the permeation ability of micelles increased 4−10-fold when the pH in the apical chamber decreased from 7.4 to 5.9, as shown in Figure 4C. The phenomena might be explained that lower pH in the apical chamber caused stronger protonation of the CS-SA micelles and larger surface charge, which enhanced the interaction ability of CS-SA micelles with a negatively charged cell surface.

Changing the added CS-SA concentration, the permeability of the micelles showed an increasing trend. The enhancement ratio ranged from 1 to 4 depending on the SD of CS-SA (Figure 3D). Though the P_{app} value increased with increasing incubation concentration, the actual increasing ratio P_{app} versus concentration was decreased, which might have suggested that saturation would be achieved with higher concentration. P_{app} of CS-SA micelles at higher concentration was not investigated mainly because that the toxicity of the micelles at higher concentration might cause an unreliable result.

3.5. Effects of Selective Endocytosis Inhibitors. Exposure of cells to different inhibitors was investigated in order to know more exactly about the possible permeation route of the micelles. Generally, colchicines and sodium azide exhibited the most significant inhibition on the permeability and uptake of the micelles across the cells. When treated with colchicines (Figure 5A), P_{app} and uptake were reduced most significantly ($p < 0.05$) by 40% and 58%, respectively. Chlorpromazine was used as an inhibitor for clathrin mediated uptake. The P_{app} and uptake were inhibited by approximately 20% and 15%, which had no significant difference with the control. Similar results were obtained when cells were coincubated with sucrose. Treatments of sodium azide resulted in a decreasing P_{app} of 15% while the uptake was inhibited by about 40%. On the contrary, the P_{app} and uptake were slightly increased in the presence of ammonium chloride.

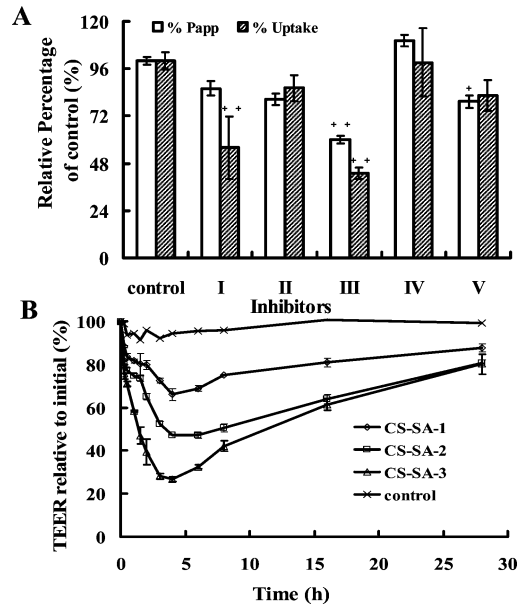

Figure 5. (A) Relative percentage of P_{app} (open bar) and cellular uptake (shaded bar) of CS-SA micelles against Caco-2 cell monolayer calculated considering the value of control groups as 100%: (I) sodium azide; (II) chlorpromazine; (III) colchicines; (IV) ammonium chloride; (V) sucrose; all the values are a mean of three parallels and are shown with error bars. + and ++ represent $P <$ 0.05 and $P < 0.01$, respectively. (B) TEER variation of Caco-2 cell monolayer after treated by different CS-SA micelles.

3.6. Effects of CS-SA Micelles on Tight Junctions. Paracellular pathway, which was mainly controlled by the tight junctions on the apical side across Caco-2 cell monolayer, was another possible route for the permeation of the chitosan-based polymer delivery system.[11,12] TEER detecting was an efficient and useful means to predict the paracellular permeability of the micelles.[19,29] The reduction of TEER between donor and receiver compartments indicates increased paracellular permeability, or the opening of intercellular tight junctions. As seen from Figure 5B, apical applications of CS-SA micelles in the Caco-2 cell monolayer led to an immediate and notable decrease in TEER values, suggesting interference of epithelial integrity and opening of tight junctions. The most significant decrease was observed of CS-SA-3 micelles by about 74%, and the smallest of CS-SA-1 micelles was decreased by about 30% of initial TEER value. After removal of the micelles and supplying with fresh DMEM medium, the TEER of the cell monolayer was recovered, which indicated a reversible opening of tight junctions of the micelles. The result suggested that the paracellular route might be another transport means of the micelles across the cell monolayer.

(29) Wang, X. D.; Meng, M. X.; Gao, L. B. Permeation of astilbin and taxifolin in Caco-2 cell and their effects on the P-gp. *Int. J. Pharm.* **2009**, *378*, 1–8.

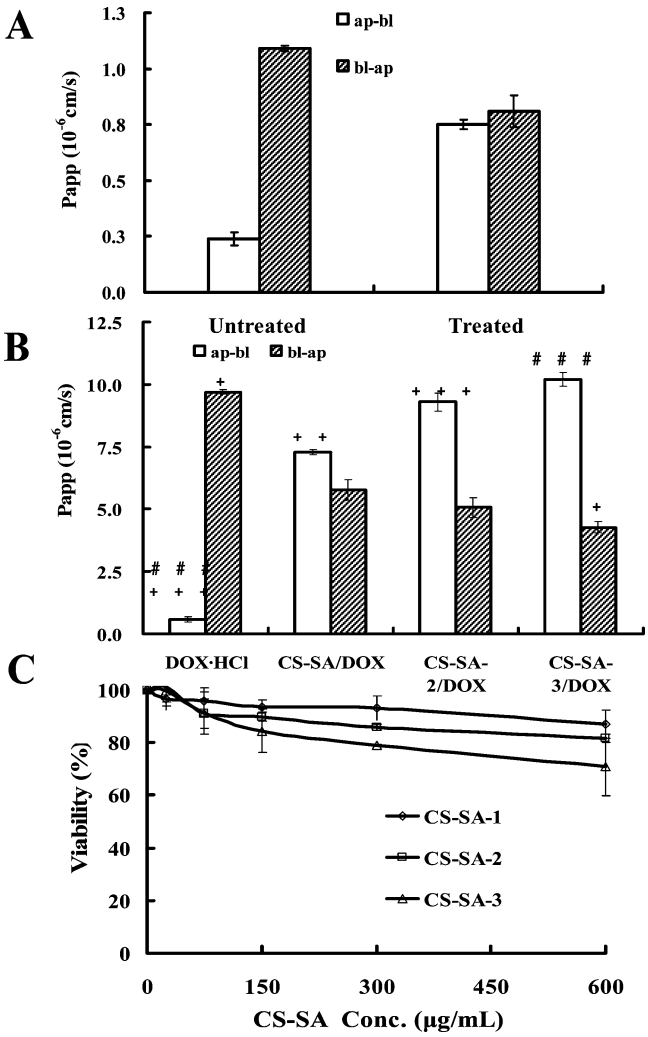

Figure 6. (A) Apparent permeability coefficient (P_{app}) of rhodamine B with or without treatment of verapamil (ap-bl, from apical to basolateral side; bl-ap, from basolateral to apical side). (B) Apparent permeability coefficient (P_{app}) of DOX·HCl and DOX for DOX·HCl solution and different CS-SA/DOX (ap-bl, from apical to basolateral side; bl-ap, from basolateral to apical side). (C) Variation of cellular viability after the cells are incubated with different CS-SA micelles having different concentrations for 4 h. + and ++, +++, ### represent $P < 0.05$ and $P < 0.01$, respectively.

3.7. Transport of DOX Encapsulated in CS-SA/DOX Micelles. Doxorubicin (DOX) was used as a model drug to investigate the potential of CS-SA micelles for facilitating drug permeation. As reported previously, DOX could be easily pumped out of the cells mediated by P-gp and the P-gp appears to be one of the major factors limiting drug absorption via the oral route.[7,47] As shown in Figure 6A, the apparent permeation coefficient of Rho B active efflux by P-gp was 3.67-fold higher than the passive influx. The ratio was decreased to 1.07-fold for cotreatment with verapamil, a typical P-gp substrate. This suggested that the used Caco-2 cells had a relatively strong P-gp pump function.

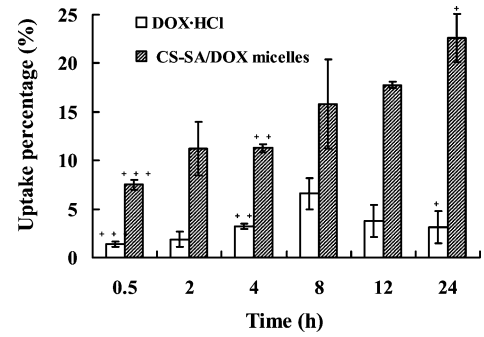

Figure 7. Cellular uptake percentages of DOX·HCl and DOX after the cells were incubated with DOX·HCl solution and CS-SA/DOX micelles for different times. + and ++, +++ represent $P < 0.05$ and $P < 0.01$, respectively.

Besides, the powerful P-gp pump efflux function was also observed in the DOX·HCl transport. As presented in Figure 6B, the absorption of DOX was significantly increased by the encapsulation of CS-SA micelles and the active efflux of DOX by P-gp pump system was decreased. The BL-AP transport of DOX for CS-SA/DOX micelles might be caused by the released DOX from the micelles. The P_{ratio} value of active absorption to efflux was enhanced 20−40-fold after the DOX loaded in CS-SA micelles, and the enhancement was increased with the SD increasing of the CS-SA micelles.

In order to explore the fact that the permeation potential of the micelles was not the result of cell structure impairment and decrease of viability, the cytotoxicity of the CS-SA micelles were investigated. According to Figure 6C, it only showed slight cytotoxic effects of CS-SA micelles with 600 μg/mL concentration (more than 70% of the cells were viable). Therefore, the good permeability of the CS-SA micelles would be attributed to their excellent mucoadhesive property and flexible transport pathway.

3.8. Cellular Uptake of CS-SA/DOX Micelles. Uptake study of CS-SA/DOX micelles was carried out to further study the CS-SA micelle intracellular uptake ability. Uptake of DOX increased with incubation time when encapsulated in CS-SA micelles (Figure 7), while it decreased in the form of DOX·HCl after 8 h incubation. Besides, the highest accumulative uptake percentage of DOX loading in CS-SA/DOX micelles was up to 22.58%, and only 6.58% was detected for DOX·HCl in the 24 h duration incubation.

3.9. In Vivo Study. Figure 8 showed the profiles of the plasma DOX concentration against time after administration of CS-SA/DOX micelles and DOX·HCl solution. In the case of oral administration of DOX·HCl solution, the plasma DOX concentrations increased at 0.5−4 h and reached peak levels, C_{max}, at 4 h. However, in the case of CS-SA/DOX micelles, peak concentration was reached at 1.5 and 6 h, which presented bimodal distribution. Moreover, the micelle delivery system maintained a long blood cycle compared with DOX·HCl solution. The key pharmacokinetic parameters, C_{max}, T_{max} AUC_{0-t}, $T_{1/2}$ and absolute bioavailability were obtained from the curves of plasma DOX concentration

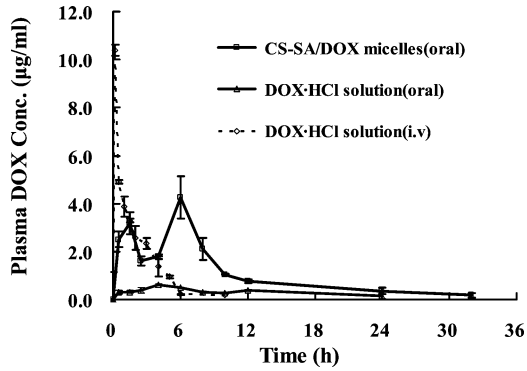

Figure 8. Plots of plasma DOX concentration against time after oral administration with different dosage form of DOX. Indicated values are the means (±SD) of three parallel animals.

Table 2. Pharmacokinetic Parameters of DOX and DOX·HCl after Intravenous Administration of DOX·HCl Solution and Oral Administration of DOX·HCl and CS-SA/DOX Micelles with a Dose of 12 mg/kg[a]

PK	DOX·HCl (iv)	DOX·HCl (oral)	CS-SA/DOX (oral)
T_{max} (h)	0.16	4.0	1.5, 6.0
C_{max} (μg/mL)	10.39 ± 1.16	0.60 ± 0.047	4.25 ± 0.89
AUC_{0-t} (μg/mL·h)	17.95 ± 0.10	8.207 ± 1.08	34.65 ± 1.40
$T_{1/2}$ (h)	1.46 ± 0.12	8.61 ± 2.94	11.21 ± 2.62
absolute bioavailability (%)		7.75 ± 1.03	25.16 ± 1.90

[a] PK: pharmacokinetics parameters. T_{max}: the time when peak plasma DOX concentration was reached. C_{max}: peak plasma DOX concentration. $T_{1/2}$: half-time of DOX eliminated in the systemic circulation. AUC_{0-t}: area under plasma DOX concentration−time curve. Each value represents the mean ± standard deviation (n = 3).

against time, and the results are summarized in Table 2. The absolute bioavailability was obtained from the calculation of AUC values between the oral administration and the iv injection of the drug at the same dose. As data presented in Table 2, the oral absolute bioavailability of CS-SA/DOX micelles was about 25.16 ± 1.90%, while the oral absolute bioavailability of DOX·HCl solution was 7.75 ± 1.03%. The relative bioavailability of CS-SA/DOX micelles was 224% higher than that of DOX·HCl solution. The half-life of the drug elimination for CS-SA/DOX micelles was extended to 11.21 h, which was prolonged compared to that of DOX·HCl solution (8.61 h). The prolonged drug elimination in blood might favor the tumor therapy. Due to the leakiness of the microvasculature in the solid tumors, the delivery system with longer blood circulation would have preferential accumulation into the tumors.[30−32] The result clearly demonstrated that the intestinal absorption of DOX was significantly improved by the encapsulation of CS-SA micelles. In addition to improved bioavailability, it also meant lower dose and lower toxicity were achieved by using the CS-SA micelle delivery system to acquire the same therapeutic effect.

4. Discussion

Oral administration of drug is the preferred route for the patient if possible. However, a number of drugs are limited for the oral route either for physiological defect or the intrinsic properties of the drug, such as poor solubility or weak permeability.[33] Strategies thus have been proposed to overcome these limitations such as the reduction of drug size,[34] salt formation,[35] or prodrug synthesis.[36] Among the approaches, encapsulation of the drug inside biodegradable nanocarriers such as nanoparticles,[37,38] polymerized liposomes,[39,40] and polymeric micelles[6−9] has now attracted extensive interest.

Particulate drug delivery systems consisting of synthesized or natural polymer were an effective approach to improve the oral absorption of drug.[7,8] Their application potential was visualized in several aspects such as improving the solubility of the drugs, increasing the fluidity of the membrane, loosening tight junctions, enhancing the drug adhesion with the cell membrane, and steric stability.[41,42] Combined with the unique properties[6−9] of polymeric micelles (hydrophilic and easily modified surface, and nano-ordered size), and the previous studies in our group,[16,17,23] the aim of this study was to elucidate whether self-assembling CS-SA polymeric micelles were able to be used as an oral drug delivery carrier.

Considering the specialty pH conditions of the GI tract, the stability of the micelles' exposure to different pH

(30) Mathot, F.; Beijsterveldt, L.; Preat, V.; Brewster, M. Intestinal uptake and bio-distribution of novel polymeric micelles after oral administration. *J. Controlled Release* **2006**, *111*, 47–55.

(31) Unezaki, S.; Maruyama, K.; Hosoda, J. I.; Nagae, I.; Koyanagi, Y.; Nakata, M.; Ishida, O.; Iwatsuru, M.; Tsuchiya, S. Direct measurement of the extravasation of polyethyleneglycol-coated liposomes into solid tumor tissue by in vivo fluorescence microscopy. *Int. J. Pharm.* **1996**, *144*, 11–17.

(32) Gabizon, A. A.; Shmeeda, H.; Zalipsky, S. Pros and cons of the liposome platform in cancer drug targeting. *J. Lipid Res.* **2006**, *16*, 175–183.

(33) Bruesewitz, C.; Funke, A.; Kuhland, U.; Wagner, T.; Lipp, R. Comparison of permeation enhancing strategies for an oral factor Xa inhibitor using the Caco-2 cell monolayer model. *Eur. J. Pharm. Biopharm.* **2006**, *64*, 229–237.

(34) Chaumeil, J. C. Micronization: a method of improving the bioavailability of poorly soluble drugs, Methods Find. *Exp. Clin. Pharmacol.* **1998**, *20*, 211–215.

(35) Serajuddin, A. T. M. Salt formation to improve drug solubility. *Adv. Drug Delivery Rev.* **2007**, *59*, 603–616.

(36) Stella, V.J. K.; Nti-Addae, W. Prodrug strategies to overcome poor water solubility. *Adv. Drug Delivery Rev.* **2007**, *59*, 677–694.

(37) Yin, Y.; Chen, D.; Qiao, M.; Lu, Z.; Hu, H. Preparation and evaluation of lectin conjugates PLGA nanoparticles for oral delivery of thymopentin. *J. Controlled Release* **2006**, *116*, 337–345.

(38) Alphandary, P. H.; Aboubakar, M.; Jaillard, D.; Couvreur, P.; Vauthier, C. Visualization of insulin-loaded nanocapsules: in vitro and in vivo studies after oral administration to rats. *Pharm. Res.* **2003**, *20*, 1071–1084.

(39) Alonso-Romanowski, S.; Chiaramoni, N. S.; Lioy, V. S.; Gargini, R. A.; Viera, L. I.; Taira, M. C. Characterization of diacetylenic liposomes as carriers for oral vaccines. *Chem. Phys. Lipids* **2003**, *122*, 191–203.

(40) Okada, J.; Cohen, S.; Langer, R. In vitro evaluation of polymerized liposomes as an oral drug delivery system. *Pharm. Res.* **1995**, *12*, 576–582.

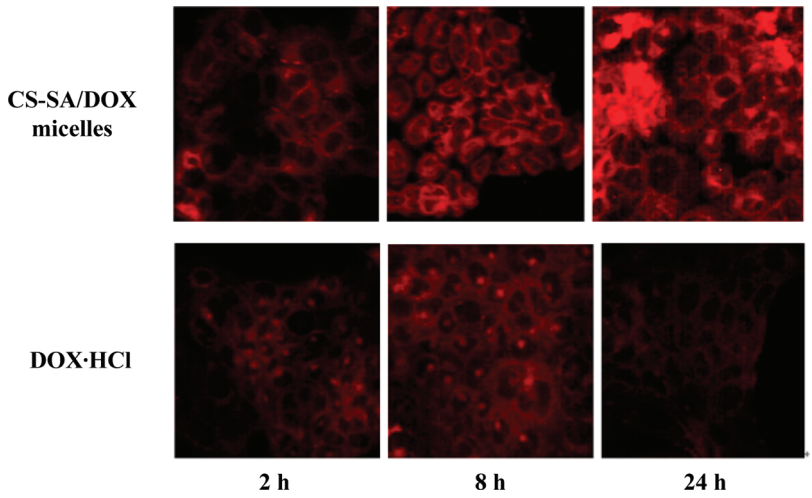

Figure 9. Fluorescent images after the cells were incubated with DOX·HCl solution and CS-SA/DOX micelles for 2, 8, and 24 h.

conditions was first investigated. The particle size, size distribution and zeta potential which were considered to have substantial effects on the stability of the nanosystem[43] were evaluated. Accordingly, basic/acid equilibrium appears to have an important impact upon aggregation,[44] and the presence of amine group in the CS molecular structure renders pH-responsiveness. As the results presented, the micelles were found to have a narrow size distribution and size variation when the incubation pH was lowered. The zeta potential was also little changed and increased with decreasing pH. This was consistent with the evidence that low pH protonated amines lead to Coulombic repulsion and curtail aggregation.[45] The higher surface charge, which contributed to a higher electrical repulsion, was favorable to the maintenance of stability. Besides, variable pK_a and CMC value of the micelles might also be responsible for its stability remaining in different pH circumstances.[8,15]

The in vitro experiment performed on Caco-2 cells suggested that CS-SA micelles had a good absorptive ability; the P_{app} was larger than 1×10^{-6} cm/s at a lower concentration. This might closely relate to the composition the special spatial structure[16,18] and the high positive surface charge of the micelles. Epithelial cells were known to possess negative charge,[46] and the mucoadhesive property of CS and positive charge induced the adherence of CS-SA micelles with epithelial cells, and the stearate branch chains near the micellar surface facilitated endocytosis of the micelles. Due to the higher permeability of the CS-SA micelles, the permeability of DOX was improved significantly via the encapsulation of CS-SA micelles. The P_{app} of DOX was increased from 5.77×10^{-7} cm/s to the range 7.28×10^{-6} to 1.02×10^{-5} cm/s.

Aside from the low permeability of the drug, the intestinal barrier caused by different transporters on the brush border membrane of intestinal epithelium such as P-glycoprotein (P-gp) was another factor to affect drug transport across the gastrointestinal tract. P-gp is an energy-dependent drug efflux pump and belongs to the family of ATP binding cassette transport proteins.[47,48] It is highly expressed on different types of tumor cells and on the apical surfaces of several epithelial (e.g., intestine) and endothelial cells (e.g., human brain capillary blood vessels that represent the blood−brain barrier).[20] It was shown in the present study that the CS-SA micelles could significantly inhibit the P-gp pump efflux (Figure 5 and Figure 9). The prolonged circulation and increased AUC of DOX·HCl after encapsulation into the micelles might also be attributed to the higher transport across the gastrointestinal tract and the inhibition of P-gp-mediated efflux of CS-SA micelles.[11]

Furthermore, we also investigated the possible factors which would affect the permeation of the micelles across

(41) Liu, J.; Zeng, F.; Allen, C. In vivo fate of unimers and micelles of poly (ethylene glycol)-block-poly (caprolactone) copolymer in mice following intravenous administration. *Eur. J. Pharm. Biopharm.* **2007**, *65*, 309–319.
(42) Yu, Q. H.; Yang, Q. Diversity of tight junctions (TJs) between gastrointestinal epithelial cells and their function in maintaining the mucosal barrier. *Cell Biol. Int.* **2009**, *33*, 78–82.
(43) Peng, Q.; Zhang, Z. R.; Sun, X.; Zuo, J.; Zhao, D.; Gong, T. Mechanisms of phospholipid complex loaded nanoparticles enhancing the oral bioavailability. *Mol. Pharmaceutics* **2010**, *7*, 565–575.
(44) Armstrong, J. K.; Chowdry, B. Z.; Snowden, M. J.; Dong, J.; Leharne, S. A. The effect of pH and concentration upon aggregation transitions in aqueous solutions of poloxamine T701. *Int. J. Pharm.* **2001**, *22*, 57–66.
(45) Dong, J.; Chowdry, B. Z.; Leharne, S. A. Solubilisation of polyaromatic hydrocarbons in aqueous solutions of poloxamine T803. *Colloids Surf., A* **2004**, *246*, 91–98.
(46) Diamond, J. M. The epithelial junction: bridge, gate, and fence. *Physiologist* **1977**, *20*, 10–18.
(47) Yang, J.; Kim, K. J.; Lee, V. H. L. Role of P-glycoprotein in restricting propranolol transport in cultured rabbit conjunctival epithelial cell layers. *Pharm. Res.* **2000**, *17*, 533–538.
(48) Orlowski, S.; Mir, J.; Belehradek, J.; Garrigos, M. Effects of steroids and verapamil on P-glycoprotein ATPase activity: progesterone, desoxycorticosterone, corticosterone and verapamil are mutually non-exclusive modulator. *Biochem. J.* **1996**, *317*, 515–522.

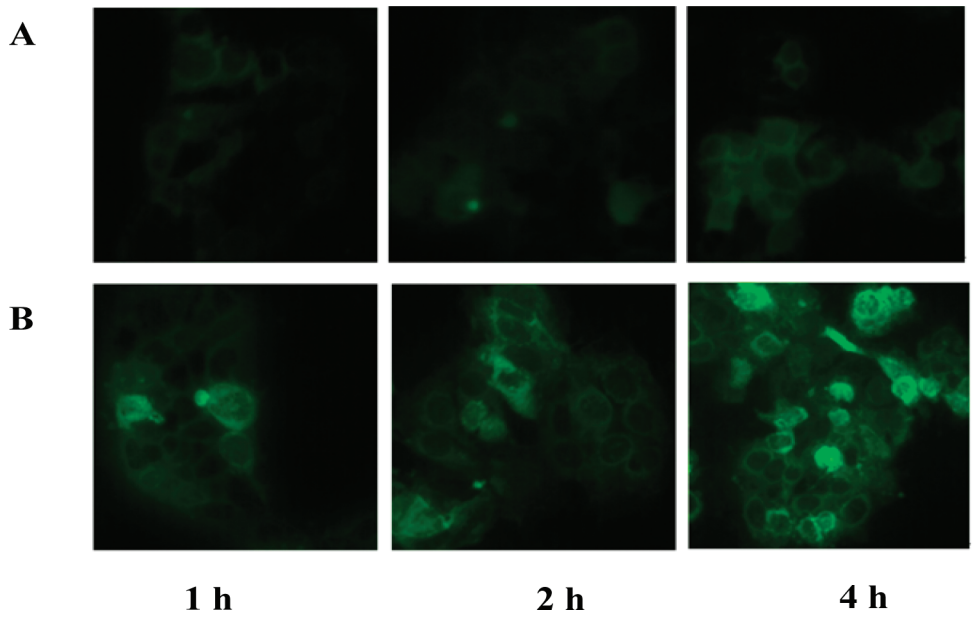

Figure 10. Fluorescence microscopic images of Caco-2 cells after incubation with the FITC labeled CS-SA micelles for 1 h, 2 and 4 h at 4 °C (A) and 37 °C (B).

the cell monolayer. It was demonstrated in the results that the micelles' permeation was significantly affected by energy, micelle concentration and medium pH. Energy dependent permeation process could also be supported by the observation of cellular uptake images. The uptake was clearly inhibited at lower temperature (4 °C) found in Figure 10. This result indicated that the micelles might internalize into cells through an active endocytosis process.[50] The endocytosis of the micelles can consume the ATP in cells, which could reduce the active efflux, and this might be the reason of the micelles to avoid the P-gp efflux pump.[20,47] However, the uptake and transport of the micelles not be completely inhibited at 4 °C. The result indicated that there were other transport pathways of the micelles such as paracellular transport and passive diffusion.[49] The transport of the CS-SA micelles was enhanced by increasing the concentration of CS-SA. However, the amounts of CS-SA micelles crossing the monolayer were not proportional to the polymer concentration applied. Indeed, the ratio of P_{app} to CS-SA concentration decreased with increasing micelle concentration. This might be due to the micelles transported via endocytosis being mainly in the form of micelles and this pathway is already saturated at concentration just above the CMC.[30] The influence of medium pH on the permeation was mainly related with the surface charge of the micelles and extracellular environment. Acidic extracellular environment was proved more favorable to the permeation of the micelles.[51] This mainly resulted from the higher positive surface charge in acid and led to an increased adhesive interaction between the micelles and the cell membrane surface.

Several studies have suggested that endocytosis, occurring most probably by fluid-phase pinocytosis,[50,52] could explain the transport of polymeric micelles across biological membranes. In order to clear the transport mechanism of the micelles, several endocytosis inhibitors were used in the study. Sodium azides[21](which block the production of ATP by interfering with the glycolytic and oxidative metabolic pathways of the cell) could inhibit the cellular metabolism. Permeation of the micelles after the sodium azide treatment was inhibited though not significantly indicating that the micelles' permeation might be an active process. Chlorpromazine inhibited clathrin mediated permeation by disrupting the assembly−disassembly of clathrin.[51,53,54] Ligands entering the cell via the clathrin pathway are believed to ultimately enter lysosomes while ligands entering the cell via a caveolar pathway do not.[55] Chlorpromazine treatment exhibited no significance difference compared with control ($p > 0.05$).

(49) Lin, Y. H.; Chung, C. K.; Chen, C. T.; Liang, H. F.; Chen, S. C.; Sung, H. W. Preparation of nanoparticles composed of chitosan/poly-gamma-glutamic acid and evaluation of their permeability through Caco-2 cells. *Biomacromolecules* **2005**, *6*, 1104–1112.

(50) Luo, L.; Tam, J.; Maysinger, D.; Eisenberg, A. Cellular internalization of poly(ethyleneoxide)-*b*-poly(ϵ-caprolactone) diblock copolymer micelles. *Bioconjugate Chem.* **2002**, *13*, 1259–1265.

(51) Pho, M. T.; Ashok, A.; Atwood, W. J. Virus enters human glial cells by clathrin-dependent receptor-mediated endocytosis. *J. Virology* **2000**, *74*, 2288–2292.

(52) Nam, Y. S.; Kang, H. S.; Park, J. Y.; Park, T. G.; Han, S. H.; Chang, I. S. New micelle-like polymer aggregates made from PEI-PLGA di-block copolymers: micellar characteristics and cellular uptake. *Biomaterials* **2003**, *24*, 2053–2059.

(53) Wang, L. H.; Rothberg, K. G.; Anderson, R. G. Mis-assembly of clathrin lattices on endosomes reveals a regulatory switch for coated pit formation. *J. Cell Biol.* **1993**, *123*, 1107–1117.

(54) Joki-Korpela, P.; Marjomaki, V.; Krogerus, C. Entry of human parechovirus 1. *J. Virology* **2001**, *75*, 1958–1967.

(55) Gabrielson, N. P.; Pack, D. W. Efficient poly-ethylenimine-mediated gene delivery proceeds via a caveolar pathway in HeLa cells. *J. Controlled Release* **2009**, *136*, 54–61.

Besides, permeation and internalization of the micelles in the presence of a hypertonic medium (sucrose), which is known as an inhibitor of clathrin-mediated endocytosis,[56] were also shown seldom inhibited compared with control group. These all suggested that clathrin might not be the main pathway of the micelle transport, which was different from the discovery by Kitchens et al.,[57] where they demonstrated that the clathrin mediated pathway was predominate in Caco-2 cells. Besides, the inhibition posed by sucrose also implied another involved pathway of the micelles endocytosis: fluid-phase endocytosis.[58] Ammonium chloride treatment increased the pH of acidic intracellular organelles such as late endosomes and lysosomes to inhibit endocytosis.[59] Thus, the endocytosis might be reduced with an increased pH of the cellular compartment. However, the result obtained was reversed, indicating that the micelles were not accessible to the endosomes. A similar result was obtained in our previous discovery that the specific core−shell spatial structure may favor the escape of CS-SA from endosome.[16] Therefore it further illustrated that the clathrin mediated pathway was not participating in the micelle transport. Colchicine is mainly contributing to the inhibition of microtubule frame structure formation, and this property is closely similar to cytochalasin,[60−62] which is involved in macropinocytosis and phagocytosis. From the result, the transport of the micelles was inhibited most significantly by colchicine treatment ($p < 0.01$), which suggested that the macropinocytosis and phagocytosis would be the dominant route of micelle transport crossing the Caco-2 cell monolayer. Besides, caveolae,[62] which mainly comprises cholesterol, mediated another important endocytosis route investigated by other study. Though the involved study on caveolar pathway was not carried out in this paper, this route could not be denied according to the result of colchicine inhibition. Given that a more complicated process was involved in the transport route, further study should be carried out to obtain a deeper understanding about the transport mechanism of the micelles.

5. Conclusions

Our results demonstrated that the CS-SA micelles were promising drug delivery vehicles in the application of oral administration. A better stability and permeability was observed of the copolymer with higher amino-substitution degree. Permeation of the micelles was an active process and mainly used micropinocytosis and phagocytosis pathway. Fluid-phase trans-cytosis and caveolar mediated pathway also possibly participated. Besides, paracellular pathway was found to be another important permeation route of the CS-SA copolymer. Further study suggested the potent ability of the CS-SA copolymer in protecting the drug from the P-gp efflux pump and improving the bioavailability, prolonging circulation time and maintaining higher concentration of the drug in the plasma.

Acknowledgment. We are grateful for financial support of National Basic Research Program of China (973 Program) under Contract 2009CB930300, National HighTech Research and Development Program (863) of China (2007AA03Z318), Zhejiang Provincial Program for the Cultivation of High-level Innovative Health talents.

MP100289V

(56) Damke, H.; Baba, T.; Bliek, A. M. V.; Schmid, S. L. Clathrin-independent pinocytosis is induced in cells over expressing a temperature-sensitive mutant of dynamin. *J. Cell Biol.* **1995**, *131*, 69–80.

(57) Kitchens, K. M.; Foraker, A. B.; Kolhatkar, R. B.; Swaan, P. W.; Eddington, N. D.; Ghandehari, H. Endocytosis and interaction of poly(amidoamine) dendrimers with Caco-2 cells. *Pharm. Res.* **2007**, *24*, 2138–2145.

(58) Emieux, B. L.; Percival, M. D.; Falgueyret, J. F. Quantitation of lysomotropic character of cationic amphiphilic drugs using the fluorescent basic amine red DND-99. *Anal. Biochem.* **2004**, *327*, 247–251.

(59) Goldman, R. The effect of cytochalasin B and colchicines on concovalin A induced vacuolization in mouse peritoneal macrophage. *Exp. Cell Res.* **1976**, *99*, 385–394.

(60) Togle, M.; Wiche, G.; Propst, F. Novel features of light chain of microtubule associated protein, MAP1B: regulation by the heavy Chain. *J. Cell Biol.* **1998**, *143*, 695–707.

(61) Nagele, R. G.; Kosciuk, M. C.; Hunter, E. T. Immuno electron microscopic localization of actin is a component of granular, microtubule associated cross bridges. *J. Brain Res.* **1998**, *474*, 279–286.

(62) Sun, F.; Li, Y. X.; Ling, Y.; Liang, L.; Chen, S.; Chen, H. P. Experimental approaches and the development of virus entry. *Microbiol. China* **2010**, *37*, 103–111.